

GRB 170817A as a jet counterpart to gravitational wave trigger GW 170817

Gavin P Lamb¹ and Shiho Kobayashi¹

¹*Astrophysics Research Institute, LJMU, IC2, Liverpool Science Park, 146 Brownlow Hill, Liverpool L3 5RF, UK*

Accepted XXX. Received YYY; in original form ZZZ

ABSTRACT

Fermi/GBM (Gamma-ray Burst Monitor) and INTEGRAL (the International Gamma-ray Astrophysics Laboratory) reported the detection of the γ -ray counterpart, GRB 170817A, to the LIGO (Light Interferometer Gravitational-wave Observatory)/*Virgo* gravitational wave detected binary neutron star merger, GW 170817. GRB 170817A is likely to have an internal jet or other origin such as cocoon emission, shock-breakout, or a flare from a viscous disc. In this paper we assume that the γ -ray emission is caused by energy dissipation within a relativistic jet and we model the afterglow synchrotron emission from a reverse- and forward- shock in the outflow. We show the afterglow for a low-luminosity γ -ray burst (GRB) jet with a high Lorentz-factor (Γ); a low- Γ and low-kinetic energy jet; a low- Γ , high kinetic energy jet; structured jets viewed at an inclination within the jet-half-opening angle; and an off-axis ‘typical’ GRB jet. The off-axis jet will produce a 10 GHz afterglow that peaks at ~ 100 days with a flux ~ 10 mJy. Only a high γ -ray efficiency low-luminosity jet, with either a high- or low- Γ , is consistent with a jet afterglow non-detection.

Key words: gamma-ray bursts: general - gravitational waves

1 INTRODUCTION

Short γ -ray bursts (GRBs) are thought to be due to internal energy dissipation (e.g. Kobayashi et al. 1997) in an ultra-relativistic jet launched when rapid accretion of material by a compact merger object occurs following a binary neutron star (NS-NS) or neutron star black hole (NS-BH) merger. The NS-NS/BH merger is due to the loss of orbital energy and angular momentum via gravitational radiation. This makes such systems a candidate for gravitational wave (GW) detection by advanced LIGO/*Virgo* (Abbott et al. 2016). The detection of a GRB in association with a GW signal is key to confirming the neutron star binary merger scenario as the progenitor for short GRBs.

GRB 170817A, with an isotropic equivalent γ -ray energy $E_\gamma = (4.0 \pm 0.98) \times 10^{46}$ erg at ~ 40 Mpc, a duration for 90% of the γ -ray energy $T_{90} \sim 2 \pm 0.5$ s, and a νF_ν spectral peak energy $E_p = 185 \pm 62$ keV (Connaughton et al. 2017; Goldstein et al. 2017a,b; Savchenko et al. 2017a,b) was detected by *Fermi*/GBM and INTEGRAL as a potential electromagnetic (EM) counterpart to the binary NS merger GW 170817 (LVC, GBM, & INTEGRAL 2017; Abbott et al. 2017) with a delay of ~ 2 s from the GW detection to the GRB. A *Swift*/UVOT detected optical counterpart was reported by Evans et al. (2017) in association with the galaxy NGC4993; the counterpart was consistent with a blue kilo/macro-nova from the dynamical merger ejecta

(e.g. Tanaka et al. 2014; Metzger et al. 2015; Tanaka 2016; Barnes et al. 2016; Wollaeger et al. 2017). If GRB 170817A was from internal dissipation within a compact merger jet then the GRB would be accompanied by an afterglow. In this paper we calculate the expected flux at various frequencies from a forward- and reverse- shock. We model the afterglow from a low-luminosity GRB jet, a low Lorentz factor (Γ) jet, structured jets with either a two-component, power-law, or Gaussian structure, and a GRB seen off-axis from a homogeneous jet with typical parameters.

In §2 the jet models and parameters used to predict the afterglows are described. In §3 we discuss the results and their implications for GRB 170817A, and in §4 we give final comments.

2 AFTERGLOW PREDICTION

Energy dissipation within an ultra-relativistic jet that results in a GRB will be followed by a broadband afterglow as the jet decelerates in the ambient medium; depending on the jet parameters, the peak magnitude and timescale at various frequencies can vary significantly. By assuming that GRB 170817A was from a compact-merger jet viewed either within or outside the jet opening angle we can make reasonable predictions for the expected afterglow. A forward-shock afterglow is expected to accompany all on-axis GRBs,

although a reverse-shock may also be present at early times and typically at low frequencies. In the following section we calculate the afterglow from forward- and reverse- shocks for a ‘classical’ GRB (e.g. Sari et al. 1998, 1999; Kobayashi & Sari 2000), and for a low-Lorentz factor jet (e.g. Lamb & Kobayashi 2016). We also calculate a forward-shock afterglow for various jet structure models viewed off the central axis, and a homogeneous jet viewed outside the jet half-opening angle (e.g. Lamb & Kobayashi 2017).

2.1 ‘Classical’ GRB: High- Γ jet

Using the main isotropic γ -ray energy reported by *Fermi* for GRB 170817A, $E_\gamma = (4.0 \pm 0.98) \times 10^{46}$ erg, and making reasonable assumptions for the afterglow parameters, a prediction can be made for the expected flux at various frequencies. The typical parameters for a sample of short GRBs are given by Fong et al. (2015) who find that the ambient density is $n \sim (3-15) \times 10^{-3} \text{ cm}^{-3}$, and the γ -ray efficiency is $0.4 \lesssim \eta \lesssim 0.7$. As the γ -ray luminosity of GRB 170817A is well below the typical values for a short GRB, we extend the efficiency range to a lower limit of 0.1. From the efficiency and γ -ray energy the jet kinetic energy can be determined, $E_k = E_\gamma(1/\eta - 1)$; the jet kinetic energy drives the afterglow. Other assumed jet parameters are the jet bulk Lorentz factor, $\Gamma = 80$, the microphysical parameters, $\varepsilon_B = 0.01$ and $\varepsilon_e = 0.1$, and the accelerated particle distribution index, $p = 2.5$.

The duration of the GRB can be used to indicate the width of the relativistic shell, $\Delta_0 \sim cT_{90}$ (Kobayashi et al. 1997), where we assume that the GRB is from internal dissipation processes and c is the speed of light. If the bulk Lorentz factor is below a critical value $\Gamma_c = (3E_k/32\pi n m_p c^2 \Delta_0^3)^{1/8}$, then the reverse shock cannot effectively decelerate the shell; here m_p is the mass of a proton. For short GRBs the reverse shock is typically described by the thin shell case. The shell crossing time for such a reverse shock is $\sim (\Gamma/\Gamma_c)^{-8/3} T_{90}$ and the characteristic frequency for the reverse shock is $\nu_{m,RS} \sim \nu_{m,FS}/\Gamma^2$ (Kobayashi 2000), where subscripts *RS* and *FS* indicate reverse- and forward- shocks respectively and $\nu_{m,FS}$ is the forward shock characteristic frequency. The spectral peak flux at the characteristic frequency is proportional to the number of electrons, the magnetic field, and the bulk Lorentz factor; the mass in the shell is a factor Γ larger than the heated and swept up ambient density of the forward shock region. The spectral peak flux for the reverse shock is then $F_{\nu,\max,RS} \sim \Gamma F_{\nu,\max,FS}$.

At low frequencies synchrotron self-absorption becomes important; for the reverse shock, synchrotron self-absorption will limit the flux more efficiently than for the forward shock because the effective temperature of the electrons in the reverse-shock region is lower by a factor of $\sim \Gamma$. The limiting flux, at a given frequency ν and observer time t , for the reverse shock is (e.g. Kobayashi & Sari 2000)

$$F_{\nu,\text{BB}} \sim 2\pi m_p c^2 \Gamma^3 D^{-2} \varepsilon_e t^2 \nu^2 \left(\frac{p-2}{p-1} \right) \max \left[\left(\frac{\nu}{\nu_m} \right)^{1/2}, 1 \right]. \quad (1)$$

For the forward shock, the limiting flux is a factor Γ larger.

The afterglow lightcurve for a jet viewed on-axis is

shown in Figure 1; the ambient density is set as the mean of the Fong et al. (2015) sample, $n = 0.009 \text{ cm}^{-3}$. Afterglow lightcurves are shown for 10 GHz, optical, and X-ray frequencies. The shaded regions represent the uncertainty in the γ -ray efficiency $0.1 \leq \eta \leq 0.7$. The bold afterglow lines show the lightcurve for a γ -ray efficiency $\eta = 0.4$, where the dashed-dotted red line is 10 GHz, the solid green line is optical ($5 \times 10^{14} \text{ Hz}$), and the dashed blue line is X-ray (10^{18} Hz). The reverse shock emission is shown as a thin dashed-dotted red line with a faint shaded region; and the reverse- and forward- shock afterglow at 10 GHz assuming the mean efficiency is shown as a thick black dashed-dotted line. The forward shock dominates emission for optical and X-ray frequencies. As a reference, the horizontal dashed-dotted line shows $1 \mu\text{Jy}$, horizontal solid line shows the $m_{\text{AB}} = 21$, and the approximate *Swift*/XRT (X-Ray Telescope) limit is given by the lower-limit of the y -axis at $10^{-32} \text{ erg cm}^{-2} \text{ s}^{-1} \text{ Hz}^{-1}$.

The forward-shock lightcurve will evolve as $t^{-3(p-1)/4}$ after the peak, and the reverse-shock lightcurve as t^{-2} . A jet viewed on-axis will exhibit a lightcurve break when $\Gamma < \theta_j$ (Sari et al. 1999), where θ_j is the jet half-opening angle. As $\Gamma \propto E_k^{1/8} n^{-1/8} t^{-3/8}$, the break time should occur at

$$t_j \sim 8.7 E_{k,50}^{1/3} n_{-2}^{-1/3} (\theta_j/0.28)^{8/3} \text{ days}, \quad (2)$$

where subscripts follow the convention $N_x = N/10^x$, θ_j is in radians and we normalise to a jet with $\theta_j = 0.28 \text{ rad}$, or $\sim 16^\circ$, the mean of the Fong et al. (2015) sample. For jets where the kinetic energy is $\lesssim 10^{48} \text{ erg}$, or the half-opening angle is $\lesssim 6^\circ$, then the jet will break at $\sim 1 \text{ day}$. Where the energy is low and the jet is narrow, then the break will occur at $\sim 0.1 \text{ days}$. As the jet half-opening angle is unknown, the jet-break is not included.

2.2 Low- Γ jet

The minimum radius at which the prompt γ -ray photons can be emitted is the photospheric radius, where the outflow becomes optically thin. The photospheric radius is given by

$$R_p = \left[\frac{\sigma_T E_k}{4\pi m_p c^2 \Gamma} \right]^{1/2} \sim 1.9 \times 10^{13} E_{k,50}^{1/2} \Gamma_1^{-1/2} \text{ cm}, \quad (3)$$

where σ_T is the Thomson cross-section.

Considering the relatively high E_p despite the low L_γ we assume that the prompt γ -ray photons are emitted near the photosphere. The observed delay time between the GW signal and the GRB is equivalent to the travel time for a constant Lorentz factor flow to a radial distance equivalent to the photospheric radius, $\Delta t \sim R_p/2\Gamma^2 c$. The bulk Lorentz factor is then

$$\Gamma = \left[\frac{(\sigma_T E_k)^{1/2}}{4\Delta t c^2 (\pi m_p)^{1/2}} \right]^{2/5} \sim 12 E_{k,50}^{1/5} \left(\frac{\Delta t}{2 \text{ s}} \right)^{-2/5}, \quad (4)$$

where Δt is the measured delay time.

The prompt emission is predicted to be suppressed for a jet with a low Lorentz factor (e.g. Hascoët et al. 2014; Lamb & Kobayashi 2016); to reflect this we extend the lower limit of the γ -ray efficiency range. The Lorentz factor for a jet with $0.001 \leq \eta \leq 0.7$, and the observed E_γ , from equation 4, is $10.0 \gtrsim \Gamma \gtrsim 2.2$. The afterglow lightcurves from low- Γ jets are shown in Figure 2; we use an efficiency of $\eta = 0.1$ for the

lightcurve. The shaded region indicates the afterglow for the limits of the efficiency.

The low- Γ value for the outflow gives a relatively long deceleration time (t_{dec}) for the jet, where $t_{\text{dec}} \propto \Gamma^{-8/3}$. The reverse shock will cross the shell at $\sim 0.4 - 1.7$ days for $10 \gtrsim \Gamma \gtrsim 2.2$ respectively. At radio frequencies the reverse-shock emission will dominate over the forward-shock lightcurve at t_{dec} for $\Gamma \gtrsim 5$. This will result in a brightening of the lightcurve before the forward-shock peak due to the reverse-shock. The reverse-shock is only important at early times and for the upper limits of the parameter space; the reverse-shock is shown for the 10 GHz lightcurves in Figure 2.

The level of suppression of the prompt emission is unknown; if all jets from binary neutron star mergers produce jets with a similar kinetic energy (e.g. Shapiro 2017), then the afterglow would appear brighter than a low-luminosity jet afterglow with a typical η value. Using a jet kinetic energy of $E_k = 10^{52}$ erg, the bulk Lorentz factor, from equation 4, would be $\Gamma \sim 30$ and the prompt emission significantly suppressed (e.g. Lamb & Kobayashi 2016). The afterglow for such a jet is shown in Figure 3; as the jet kinetic energy is fixed, here the limits of the shaded regions represent the uncertainty on the ambient medium number density, $n \sim (3 - 15) \times 10^{-3} \text{ cm}^{-3}$. A reverse-shock is apparent at 10 GHz, peaking at ~ 0.6 days with a flux ~ 10 Jy; the reverse-shock is shown in the figure as a thin red dashed-dotted line with the associated uncertainty in the ambient number density. A black dashed-dotted line indicates the sum of the 10 GHz lightcurve from the forward- and reverse- shocks.

2.3 Structured Jet

GRBs are usually assumed to have a homogeneous, or ‘top-hat’, structure i.e. the energy and Lorentz factor are uniform in a jet cross-section and the jet has a sharp edge defined by the jet half-opening angle. However, jets may have some intrinsic structure either due to the formation and acceleration processes or as a result of jet breakout from merger ejecta. Here we use the structured jet models from Lamb & Kobayashi (2017); see also Xiao et al. (2017) for a similar analysis. For each of the three models used the total isotropic equivalent jet core energy is fixed at 10^{52} erg, and the core extends to an angle of 6° from the central axis. The jet parameters, E and Γ , vary according to the model: for a two-component jet, E and Γ are at 5% of the core values between $(6 - 25)^\circ$; for a power-law jet, E and Γ vary with angle outside the core following a power-law index -2; and for a Gaussian structured jet the parameters E and Γ depend on angle following a Gaussian function from $(0 - 25)^\circ$. The detected prompt emission in a 50-300 keV band is determined for each jet model at observation angles from $(0 - 25)^\circ$ and a distance 40 Mpc. The observation angle values are selected for each jet structure where the detected prompt photon flux is comparable to the observed *Fermi*/GBM and INTEGRAL. The afterglow from each model for the determined inclination is then generated following the method in Lamb & Kobayashi (2017).

The Gaussian jet model, shown in Figure 4 left panel, has an inclination of 14.5° . For the power-law jet model, shown in Figure 4 central panel, the inclination angle is 23.5° . For the two-component model, shown in Figure 4 right

panel, the inclination angle is 8.5° ; note that for the two-component model the γ -ray emission is that seen off-axis from the core jet region, the wider sheath component has a low- Γ value such that the prompt emission is fully suppressed. In the figure the afterglow at 10 GHz is shown in red with a dashed-dotted line, optical is shown in green with a solid line, and X-ray is shown in blue and with a dashed line. The shaded region represents the uncertainty in the ambient medium number density, with the line indicating the afterglow for the mean $n = 0.009 \text{ cm}^{-3}$.

For each model the first break in the lightcurve is due to the deceleration time for the jet component inclined towards the observer, i.e. the jet-component at the inclination angle. At radio frequencies, the lightcurve will peak when the characteristic frequency crosses the observation band, $\nu_m = \nu$. At optical and X-ray frequencies, and at radio frequencies for the two-component jet, a late-time excess or a shallow decay is due to the off-axis emission from the bright core of the jet. Any late-time break in the lightcurve is due to the edge of the jet becoming visible i.e. the jet-break, equation 2.

For the structured jet models the photon flux at the detector from the prompt emission approximates, without fine-tuning, the observed parameters: for the two-component jet the prompt fluence is $\sim 3.5 \times 10^{-7} \text{ erg cm}^{-2}$ with a $T_{90} \sim 2.0$ s; for the power-law jet the prompt fluence is $\sim 2.8 \times 10^{-7} \text{ erg cm}^{-2}$ with a $T_{90} \sim 1.9$ s; and for the Gaussian jet the prompt fluence is $\sim 2.5 \times 10^{-7} \text{ erg cm}^{-2}$ with a $T_{90} \sim 1.7$ s. The *Fermi*/GBM measured fluence is $(2.8 \pm 0.2) \times 10^{-7} \text{ erg cm}^{-2}$ (Goldstein et al. 2017b) with a $T_{90} = 2 \pm 0.5$ s (LVC, GBM, & INTEGRAL 2017). The difference in fluence between the jet models and the observed value is due to the choice of numerical resolution. The fluence for each jet model was calculated in 0.5° steps from $0 - 25^\circ$ and the inclination for the jet determined by the angle for which the fluence was closest to the observed value.

2.4 Off-Axis Afterglow

The T_{90} duration of GRB 170817A is longer than the typical value of ~ 0.6 s (Zhang et al. 2012), although still within the usual period for short GRB classification $\lesssim 2$ s. The delay time between the GW signal and the detected prompt emission, and the duration and low-luminosity of the γ -rays could be due to the jet inclination to the line-of-sight; where for an off-axis observer the time until emission and the duration are lengthened from that for an on-axis observer by the relativistic Doppler factor, $t \propto \delta^{-1}$ where t is the observed time, $\delta = [\Gamma(1 - \beta \cos \theta_{\text{obs}})]^{-1}$ is the Doppler factor and β the velocity as a fraction of c , and the observed fluence is $\propto \delta^3$ (e.g. Ioka & Nakamura 2001). The off-axis prompt emission will also appear to be brighter in X-rays (e.g. Yamazaki et al. 2002).

If the jet is inclined in such a way that the observer’s line-of-sight is outside of the jet edge i.e. $\theta_{\text{obs}} > \theta_j$, then the prompt and afterglow emission will be delayed and suppressed when compared to that seen by an on-axis observer i.e. $\theta_{\text{obs}} \rightarrow 0$. In considering an observer at various angles from the jet central axis, we use the method in Lamb & Kobayashi (2017) which includes the jet geometry and emission surface to determine the inclination at which the

prompt γ -ray photons have a similar fluence and timescale¹. At an inclination of 8.5° for a jet with $\theta_j = 6^\circ$, $E_{\text{iso}} = 10^{52}$ erg, an efficiency $\eta = 0.4$, and a $\Gamma = 80$, the simplest estimate of the fluence in a T_{90} period from our model is 4.0×10^{-7} erg cm $^{-2}$ and $T_{90} = 2.2$ s. The corresponding afterglow in an ambient medium $0.003 \leq n \leq 0.015$ cm $^{-3}$ is shown in Figure 5 where the colours are as previous figures. Note that as $\nu_a < \nu < \nu_m$ at the deceleration time for the 10 GHz lightcurve, then the synchrotron self-absorption frequency $0.25 \lesssim \nu_a \lesssim 0.75$ GHz at this time will not affect the lightcurve (Sari et al. 1999).

Given an observed $E_p \sim 185$ keV, and the inclination, jet half-opening angle and Γ used, the ‘on-axis’ spectral peak energy would be a few MeV. Short GRBs with a spectral peak of a few MeV include GRB 061006, 070714, and 090510; where the $E_p = [955 \pm 267, 2150 \pm 1113, \text{ and } 8370 \pm 760]$ keV respectively (e.g. Zhang et al. 2012; Piron 2016). All of these GRBs have high luminosities for short GRBs, where $L_\gamma > 10^{52}$ erg s $^{-1}$. Our choice of $\Gamma = 80$ is motivated by this; if the Lorentz factor for the jet viewed off-axis was > 100 , then the required inclination would be much lower and the observed afterglow would be earlier and brighter than that shown in Figure 5.

3 DISCUSSION

By assuming that the observed GRB is from a compact merger jet we have shown the expected afterglow lightcurves for various jet models. If GRB 170817A was a low-luminosity GRB viewed on-axis, the afterglow in X-ray and optical would peak within seconds of the GRB. A reverse-shock in the radio, typically fainter than $\lesssim 1$ mJy at 10 GHz, will be visible peaking on a timescale of a minute; this will be followed by the radio forward-shock afterglow peak with flux $\lesssim 0.1$ mJy at ~ 1 day i.e. Figure 1. The predicted optical afterglow is fainter than $m_{AB} \lesssim 19$, and the X-ray afterglow is detectable by *Swift*/XRT but will fade rapidly. The X-ray afterglow will peak within seconds and typically last ~ 15 minutes before becoming too faint for *Swift*/XRT, where we assume an X-ray limit of $> 10^{-32}$ erg cm $^{-2}$ s $^{-1}$ Hz $^{-1}$. Such a fast and faint transient would be challenging to detect.

By considering the delay time from GW signal to GRB, constraints can be put on the jet bulk Lorentz factor, if the jet is inclined within the half-opening angle i.e. on-axis. The energy dissipated will decouple from the jet when the optical depth becomes unity, at the photospheric radius. By using an assumed γ -ray efficiency, the jet kinetic energy can be estimated and from this and the delay time a value for Γ found. The bulk Lorentz factor found using an efficiency $0.001 \leq \eta \leq 0.7$ is $10.0 \geq \Gamma \geq 2.2$ respectively. This is consistent with the low- Γ jet model of Lamb & Kobayashi (2016) where the prompt emission is expected to be significantly suppressed. The forward shock afterglow from such a jet is shown in Figure 2; the afterglow peak in all bands is

$\lesssim 1$ day and optical and X-ray are faint. Radio at 10 GHz is typically $\lesssim 1$ mJy, and would be detectable for $\gtrsim 1 - 100$ days.

If the γ -ray efficiency is very low i.e. the jet kinetic energy is $E_k \gg E_\gamma$ then the derived bulk Lorentz factor, using $E_k = 10^{52}$ erg, is $\Gamma \sim 30$. This value is consistent with the low- Γ jet model, predicting significant suppression of the prompt emission resulting in a low-luminosity GRB. The afterglow for such a jet is shown in Figure 3; the peak afterglow is typically a few hours after the GRB at optical and X-ray frequencies. Radio, optical, and X-ray emissions are bright in all cases. The 10 GHz afterglow remains at the ~ 1 Jy level for $\sim 10 - 1000$ days, while optical and X-ray fade rapidly.

A jet with extended structure may naturally produce low-luminosity GRBs at wider angles where the jet energetics are lower. By following the structured jet models of Lamb & Kobayashi (2017), we show the expected afterglow from a jet with these models where the observed γ -ray flux is equivalent to the detected *Fermi* value. The afterglows from a Gaussian jet viewed at $i = 14.5^\circ$, a power-law jet viewed at $i = 23.5^\circ$, and a two-component jet viewed at an inclination $i = 8.5^\circ$ are shown in Figure 4. Radio, optical and X-ray emissions are bright in all cases with optical and X-ray lightcurves peaking ~ 1 day, and 10 GHz at $10 - 100$ days at the 0.1-1 Jy level. Various features are distinct for each jet model: the Gaussian jet has an early peak with a shallow decline in optical and X-ray emission for ~ 100 days before breaking to a more rapid decline. In addition the radio peaks significantly later than the optical and X-ray lightcurves. The power-law jet has a sharp early peak at optical and X-ray frequencies whilst the 10 GHz afterglow has a later peak with a slow increase in flux after the deceleration time. Finally the two-component jet has a softer peak and shows a slight rebrightening at late times, especially at radio frequencies, before a rapid decline.

An observer at an inclination just higher than the jet’s half-opening angle will see the relativistically beamed prompt and afterglow emission at a later time and at a lower frequency and intensity. The observed delay in the prompt emission, and the low-luminosity can be explained by the jet inclination; the afterglow in such a case would be similarly delayed and fainter. We show the afterglow for an observer at 8.5° from the jet central axis, where the jet has a half-opening angle $\theta_j = 6^\circ$, an isotropic equivalent blast energy 10^{52} erg, a γ -ray efficiency of $\eta = 0.4$, and $\Gamma = 80$. The X-ray afterglow, at ~ 4 keV, is faint and rises slowly to a peak flux $\lesssim 10^{-32}$ erg cm $^{-2}$ s $^{-1}$ Hz $^{-1}$ at ~ 100 days; optical afterglow has a similar rise index and peak time with a $m_{AB} \lesssim 20$; while the 10 GHz afterglow has a steeper rise rate, breaking to a soft peak from 60 days, the 10 GHz afterglow is brighter than $1 \mu\text{Jy}$ from $\gtrsim 10 - 20$ days and peaks at ~ 10 mJy.

A neutron star binary merger is expected to produce a kilo/macro-nova that will peak with a thermal spectrum at optical to near-infrared frequencies during the first 10 days (e.g. Tanaka et al. 2014; Metzger et al. 2015; Tanaka 2016; Barnes et al. 2016; Wollaeger et al. 2017). For the structured jet afterglows, the optical emission will peak on a similar timescale to any expected kilo/macro-nova. However X-ray and radio emission will reveal the afterglow in such a case. Non-detections by X-ray and/or radio searches for an afterglow from GRB 170817A at these times can be used

¹ We do not change any of the prompt energy parameters from the model in Lamb & Kobayashi (2017) except the total isotropic energy, efficiency, and bulk-Lorentz factor, where we use $E = 10^{52}$ erg, $\eta = 0.4$ and $\Gamma = 80$ instead of $E = 2 \times 10^{52}$ erg, $\eta = 0.1$ and $\Gamma = 100$. This maintains consistency with earlier scenarios and avoids fine-tuning.

to rule out the various structured, and high kinetic energy with low- Γ jet scenarios in this case.

The prompt emission for GRB 170817A was fit by an exponential cut-off power-law, the Comptonization spectrum model (e.g. Yu et al. 2016), with a νF_ν spectral peak energy at $E_p \sim 185 \pm 62$ keV and an index $\alpha \sim -0.62 \pm 0.40$ (Connaughton et al. 2017; Goldstein et al. 2017a,b). Due to the sparsity of high-energy photons, the requirement for an ultra-relativistic bulk Lorentz factor is relaxed. Additionally, with this E_p and low luminosity the GRB does not fit on the $E_p - L_\gamma$ correlation for all GRBs (e.g. Yonetoku et al. 2010; Zhang et al. 2012). The detected γ -ray flux may not have been from within the jet i.e. internal dissipation; the prompt emission could be from wider angle Comptonized emission; either a cocoon or shock-breakout (Nakar & Piran 2017; Lazzati et al. 2017), or a flare due to fragmentation of a viscous disc (Perna et al. 2006) seen at a much higher inclination.

4 CONCLUSIONS

We have modelled the afterglow from various jet dynamical scenarios given the observed γ -ray flux detected by *Fermi* and INTEGRAL for GRB 170817A in association with the GW signal GW 170817. Four scenarios were considered: (i) an on-axis low-luminosity GRB with typical high Lorentz factor; (ii) low- Γ jets viewed on-axis; (iii) jets with extended structure where the prompt emission would have an energy and timescale similar to that observed; (iv) and an off-axis jet where the prompt emission is geometrically corrected to give the observed γ -ray flux. In all cases an afterglow is expected on various timescales and with a range of peak fluxes. Where the kinetic energy is typical for a GRB jet, the afterglow for either a low- Γ jet or from a structured jet where the prompt γ -ray emission is suppressed or low, will result in a bright afterglow, easily detectable at all frequencies. If GRB 170817A is from within a relativistic jet then the jet must be either:

- A low energy jet with either a low- or high- Γ , and a high γ -ray efficiency $\eta \gtrsim 0.4$
- Or a typical GRB jet viewed just off-axis

If the jet is the first of these, then a large population of low-luminosity, low-energy jets from neutron star mergers could exist resulting in a high GW detection rate for neutron star mergers.

A jet viewed off-axis will produce an afterglow that will peak at ~ 100 days, radio and optical will be brightest although a sensitive X-ray telescope (e.g. Chandra) may be able to make the detection. If the off-axis afterglow is not detected, then the origin of GRB 170817A is either a low-luminosity low-energy jet (where a low- Γ can explain the observed Δt), or not from a merger jet. A radio counterpart was reported by the VLA at 3 and 6 GHz on the 2-3 September, ~ 18 days after the GW signal (Hallinan, Corsi et al. 2017; Mooley, Hallinan & Corsi 2017; Corsi et al. 2017); however, radio counterparts are expected from the merger ejecta at late times (e.g. Hotokezaka et al. 2016) and continued observation will reveal if this is due to an off-axis jet afterglow, where the flux should increase until a peak at $\gtrsim 60$ days.

ACKNOWLEDGEMENTS

This research was supported by STFC grants. The authors thank Iain A. Steele, Phil James, and Dan Hoak for useful comments.

REFERENCES

- Abbott, B. P., Abbott, R., Abbott, T. D., et al. 2016, *Living Reviews in Relativity*, 19, 1
- Abbott, B. P., et al., (LIGO Scientific Collaboration and Virgo Collaboration) 2017, *Phys. Rev. Lett.*, 119, 161101
- Barnes, J., Kasen, D., Wu, M.-R., & Martínez-Pinedo, G. 2016, *ApJ*, 829, 110
- Connaughton, V., Blackburn, L., Briggs, M.S., et al. 2017, *GCN* 21506
- Corsi, A., Hallinan, G., Mooley, K., et al. 2017, *GCN* 21815
- Evans, P. A., Kennea, J. A., Breeveld, A. A., et al. 2017, *GCN* 21550
- Fong, W., Berger, E., Margutti, R., & Zauderer, B. A. 2015, *ApJ*, 815, 102
- Goldstein, A. et al. 2017, *ApJ*, (submitted)
- Goldstein, A., Veras, P., von Kienlin, A., et al. 2017, *GCN* 21528
- Hallinan, G., Corsi, A., et al. 2017, (submitted)
- Hascoët, R., Beloborodov, A. M., Daigne, F., & Mochkovitch, R. 2014, *ApJ*, 782, 5
- Hotokezaka, K., Nissanke, S., Hallinan, G., et al. 2016, *ApJ*, 831, 190
- Ioka, K., & Nakamura, T. 2001, *ApJ*, 554, L163
- Kobayashi, S., Piran, T., & Sari, R. 1997, *ApJ*, 490, 92
- Kobayashi, S., & Sari, R. 2000, *ApJ*, 542, 819
- Kobayashi, S. 2000, *ApJ*, 545, 807
- Lamb, G. P., & Kobayashi, S. 2016, *ApJ*, 829, 112
- Lamb, G. P., & Kobayashi, S. 2017, *MNRAS*, (accepted)
- Lazzati, D., Deich, A., Morsony, B. J., & Workman, J. C. 2017, *MNRAS*, 471, 1652
- LVC, GBM, & INTEGRAL. 2017, *ApJ*, (accepted)
- Metzger, B. D., Bauswein, A., Goriely, S., & Kasen, D. 2015, *MNRAS*, 446, 1115
- Mooley, K. P., Hallinan, G., & Corsi, A. 2017, *GCN* 21814
- Nakar, E., & Piran, T. 2017, *ApJ*, 834, 28
- Perna, R., Armitage, P. J., & Zhang, B. 2006, *ApJ*, 636, L29
- Piron, F. 2016, *Comptes Rendus Physique*, 17, 617
- Sari, R., Piran, T., & Narayan, R. 1998, *ApJ*, 497, L17
- Sari, R., Piran, T., & Halpern, J. P. 1999, *ApJ*, 519, L17
- Savchenko, V. et al. 2017, *ApJ*, (submitted)
- Savchenko, V., Mereghetti, S., Ferrigno, C., et al. 2017, *GCN* 21507
- Shapiro, S. L. 2017, *Phys. Rev. D*, 95, 101303
- Tanaka, M., Hotokezaka, K., Kyutoku, K., et al. 2014, *ApJ*, 780, 31
- Tanaka, M. 2016, *Advances in Astronomy*, 2016, 634197
- Wollaeger, R. T., Korobkin, O., Fontes, C. J., et al. 2017, *arXiv:1705.07084*
- Xiao, D., Liu, L.-D., Dai, Z.-G., & Wu, X.-F. 2017, *arXiv:1710.00275*
- Yamazaki, R., Ioka, K., & Nakamura, T. 2002, *ApJ*, 571, L31
- Yonetoku, D., Murakami, T., Tsutsui, R., et al. 2010, *PASJ*, 62, 1495
- Yu, H.-F., Preece, R. D., Greiner, J., et al. 2016, *A&A*, 588, A135
- Zhang, F.-W., Shao, L., Yan, J.-Z., & Wei, D.-M. 2012, *ApJ*, 750, 88

This paper has been typeset from a \LaTeX file prepared by the author.

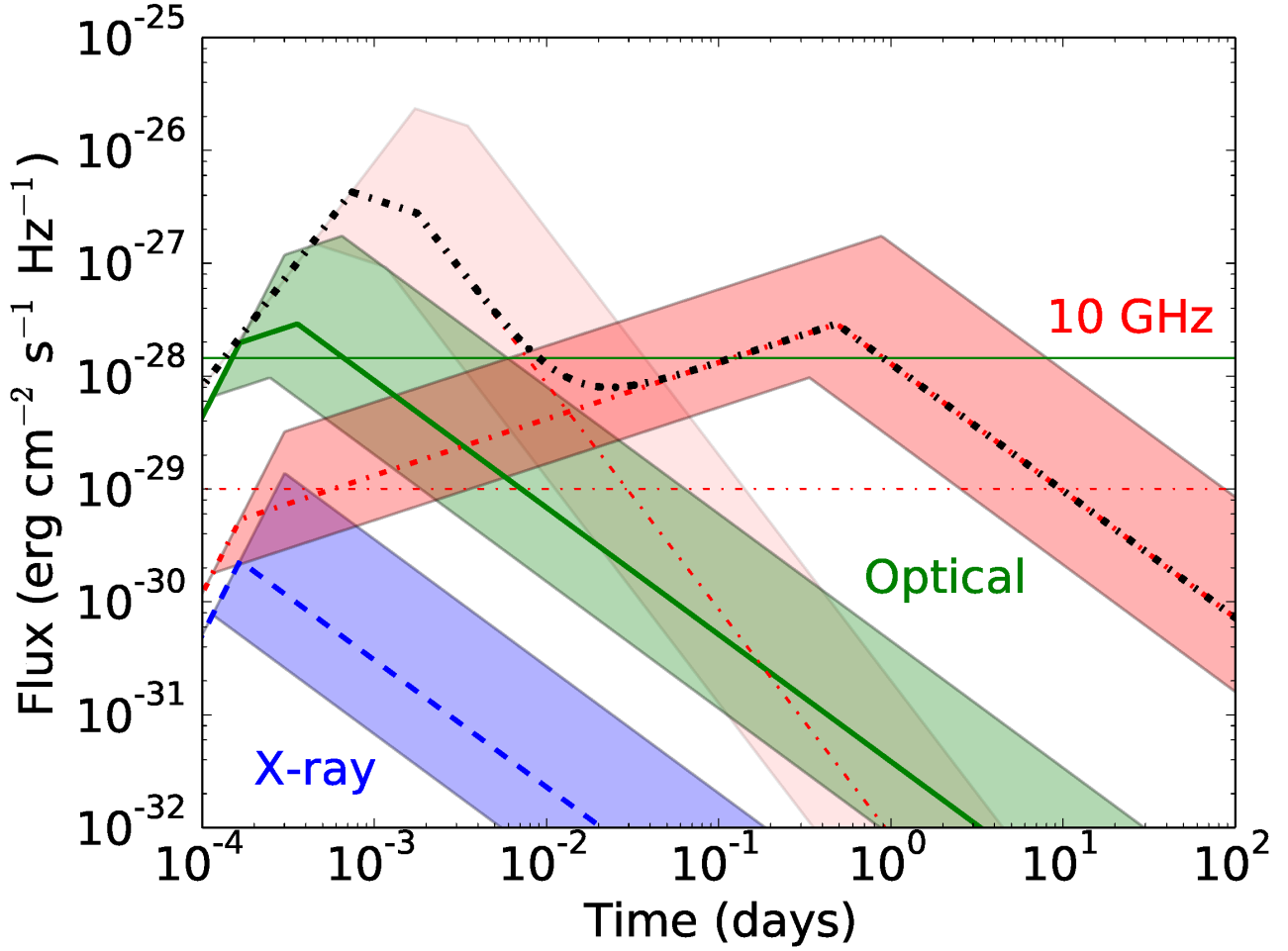


Figure 1. Afterglow lightcurves for a jet with an isotropic γ -ray energy of 4.0×10^{46} erg, a γ -ray efficiency of $\eta = 0.4$, a jet bulk Lorentz factor $\Gamma = 80$, in an ambient medium of $n = 0.009 \text{ cm}^{-3}$ with microphysical parameters $\varepsilon_B = 0.01$ and $\varepsilon_e = 0.1$, and a luminosity distance of 40 Mpc. The blue dashed line shows the X-ray afterglow, the green solid line shows the optical afterglow, and the red dashed-dotted line shows the 10 GHz radio afterglow. The shaded regions indicate the lightcurve for an efficiency $0.1 \leq \eta \leq 0.7$. The reverse shock is important at radio frequencies, the 10 GHz reverse shock is shown as a thin dash-dotted red line and faint shaded region for the range of jet energies considered; the forward and reverse shock lightcurve at 10 GHz is shown as a thick black dashed-dotted line. The red dashed horizontal line indicates the $1 \mu\text{Jy}$ limit, the green horizontal dashed line indicates $m_{AB} \sim 21$ magnitude, and lower-limit of the y -axis is the X-ray sensitivity $\sim 0.4 \mu\text{Crab}$ at 4 keV

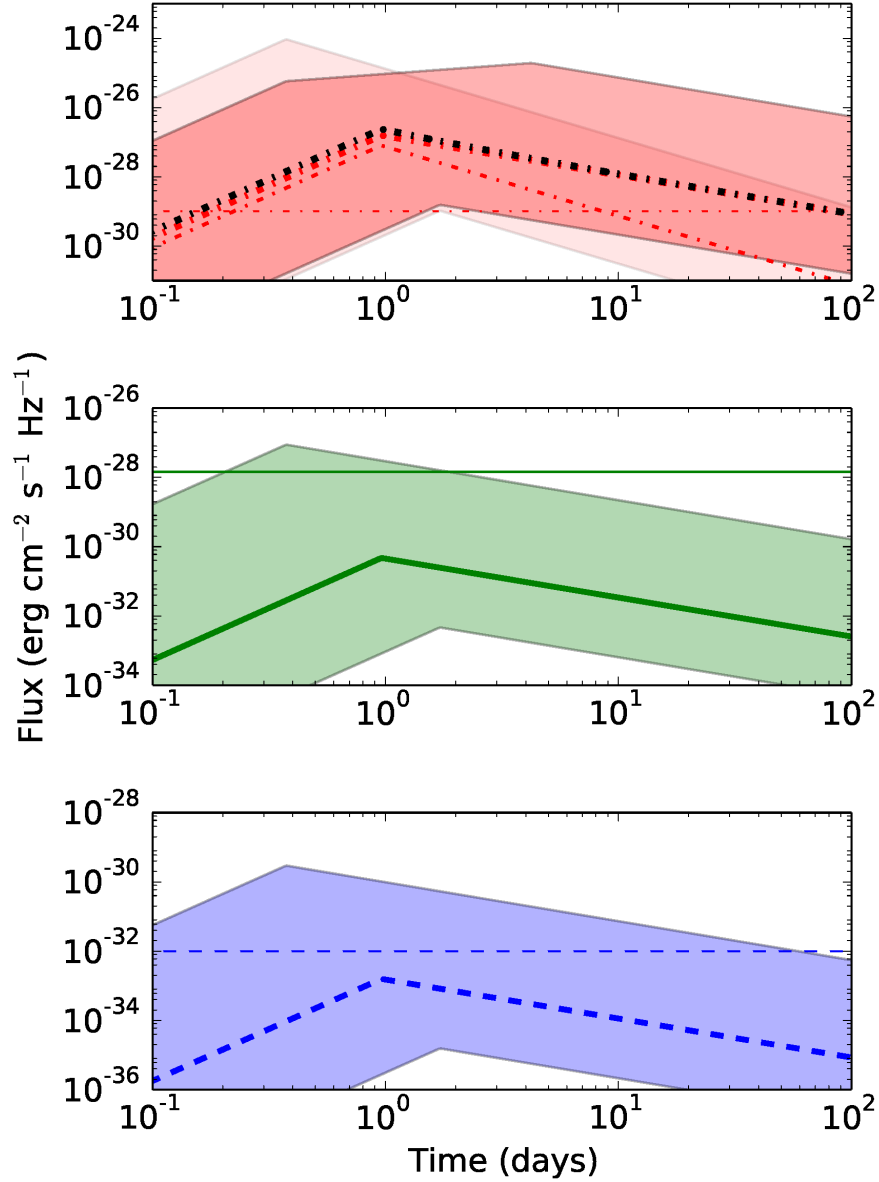


Figure 2. Afterglow from a low- Γ jet with an isotropic γ -ray energy of 4.0×10^{46} erg, a γ -ray efficiency of $0.001 \leq \eta \leq 0.7$ and a luminosity distance 40 Mpc. The jet bulk Lorentz factor is estimated from the delay time as $2.2 \lesssim \Gamma \lesssim 10.0$, all other parameters are as Figure 1. The lines show the afterglow for a jet with $\Gamma \sim 3.9$, the shaded regions indicate the uncertainty in the kinetic energy and the Lorentz factor. Colours are as for figure 1. **Top** panel: 10 GHz emission where the thin dashed-dotted line and faint shaded region indicate the reverse-shock; the thick dashed-dotted line and shaded region indicate the forward-shock; the sum of reverse- and forward-shock light-curves is shown as a black dashed-dotted line. The red horizontal dashed line indicates the $1 \mu\text{Jy}$ limit. **Middle** panel: optical afterglow. The green solid line shows the optical magnitude 21. **Bottom** panel: X-ray afterglow. The blue horizontal dashed line is $\sim 0.4 \mu\text{Crab}$ at ~ 4 keV

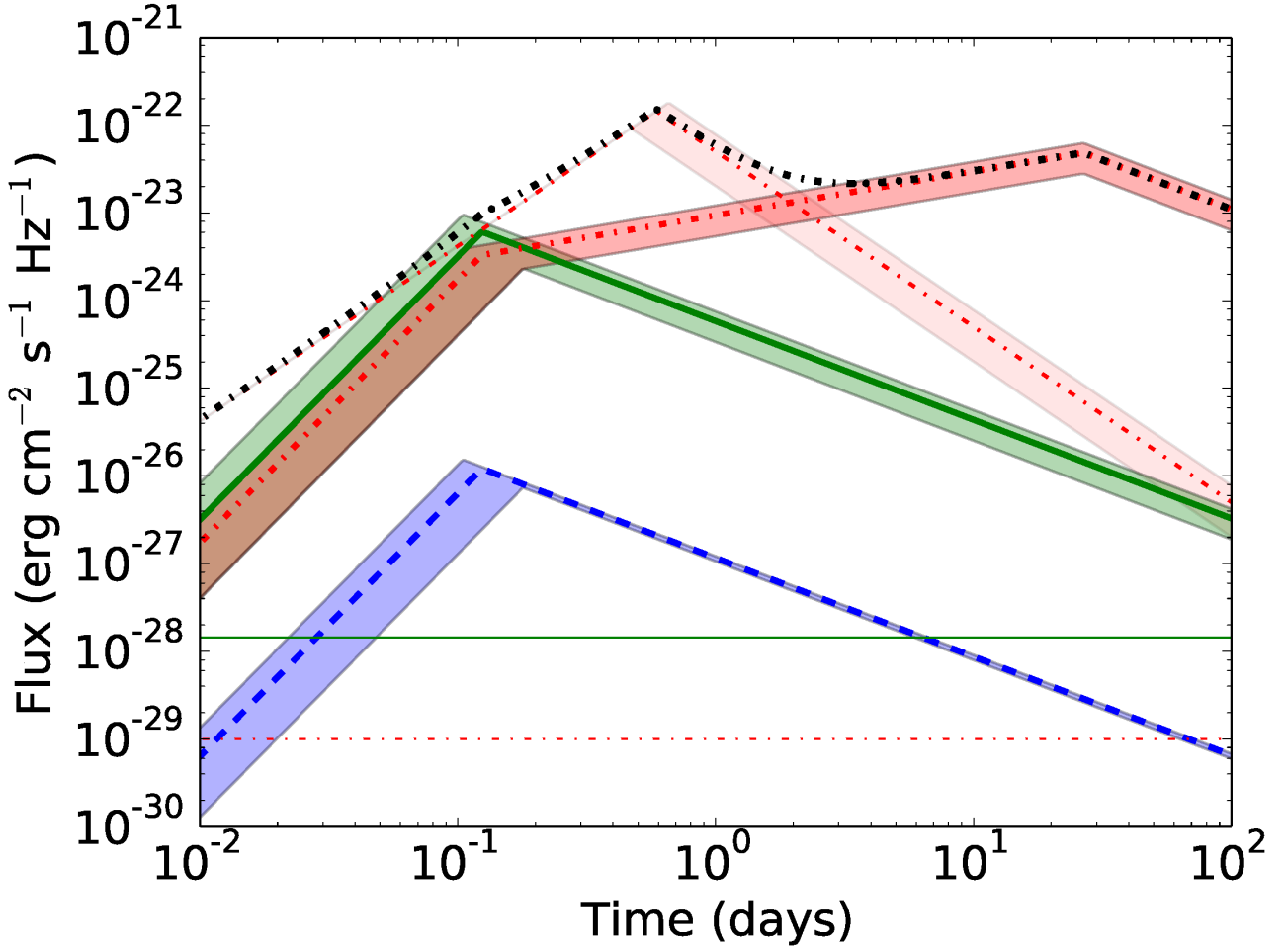


Figure 3. Afterglow from a low- Γ jet with a jet kinetic energy of 10^{52} erg, and a luminosity distance 40 Mpc. The jet bulk Lorentz factor is estimated from the delay time as $\Gamma \sim 30$. Shaded regions represent the range of ambient densities ($3 \lesssim n \lesssim 15$) $\times 10^{-3} \text{ cm}^{-3}$, all other parameters are as Figure 1. The reverse-shock at 10 GHz is shown as a thin dash-dotted red line and faint shaded region. Colours are as for Figure 1. The green horizontal solid line is optical $m_{AB} = 21$, and the red horizontal dashed-dotted line indicates the $1 \mu\text{Jy}$ limit

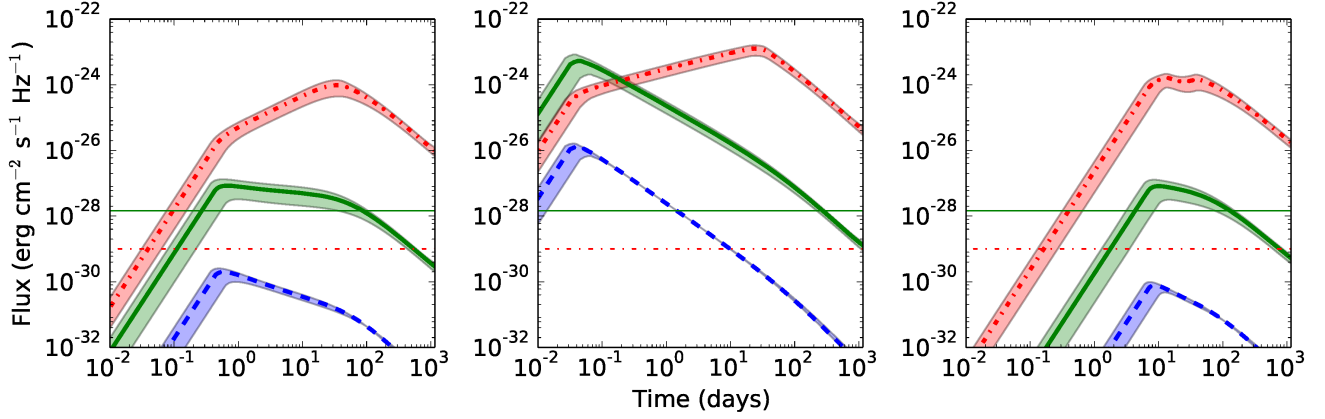


Figure 4. Afterglows from jets with structure; jet core parameters are $E_{\text{iso}} = 10^{52}$ erg, $\eta = 0.4$, $\Gamma = 80$, and $\theta_c = 6^\circ$, all other parameters are as previously used. The jet structure extends to 25° in each case. **Left:** Gaussian structure, a Gaussian function on E and Γ with angle from the centre. Jet inclined to the observer at 14.5° . **Middle:** Power-law structure with a decay index outside of the core of $k = -2$. Jet inclined to the observer at 23.5° . **Right:** Two-component structure, where the second component has 5% of the core parameters. Jet inclined to the observer at 8.5° .

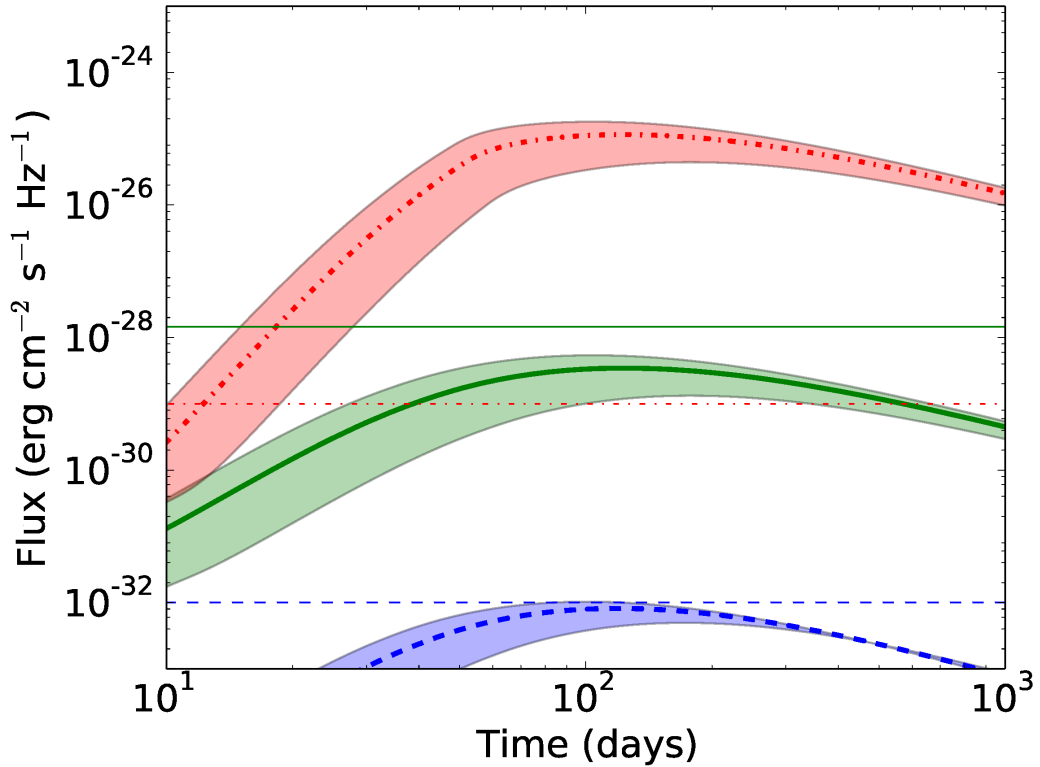


Figure 5. Off-axis afterglow from a homogeneous jet with $E_{\text{iso}} = 10^{52}$ erg, $\eta = 0.4$, $\Gamma = 80$, and a half-opening angle $\theta_j = 6^\circ$. The observed γ -ray fluence in the 50–300 keV band is 4.0×10^{-7} erg cm $^{-2}$ in a $T_{90} = 2.2$ s; the inclination from the jet central axis is 8.5° and the ambient density is in the range $0.003 \leq n \leq 0.015$ cm $^{-3}$.